Sensitivity of typhoon-induced gravity waves to cumulus parameterizations

So-Young Kim,[1] Hye-Yeong Chun,[1] and Jong-Jin Baik[2]

Received 5 May 2007; revised 21 June 2007; accepted 20 July 2007; published 15 August 2007.

[1] Sensitivity of typhoon-induced gravity waves to cumulus parameterizations is examined using a mesoscale model (MM5). For this, Typhoon Rusa (2002) is simulated with four cumulus parameterizations (Kain-Fritsch, Grell, Anthes-Kuo, and Betts-Miller schemes) and the characteristics of typhoon-induced gravity waves are compared. The experiments show differences in rainband structure and vertical motion, resulting in different forcing spectra for zonal wavelength and period. As a result, induced stratospheric gravity waves are different in amplitude and spectral shape. However, the difference is not as large as that in the forcing spectrum, since a large portion of the waves generated by major forcing components is filtered out by the background wind, which is nearly the same in all the experiments. Instead, variation in zonal wavelength and period of forcing modifies the characteristics of stratospheric gravity waves by changing damping time scale in the nonfiltered region. **Citation:** Kim, S.-Y., H.-Y. Chun, and J.-J. Baik (2007), Sensitivity of typhoon-induced gravity waves to cumulus parameterizations, *Geophys. Res. Lett.*, *34*, L15814, doi:10.1029/2007GL030592.

1. Introduction

[2] It is known that nonstationary gravity waves play an important role in the momentum budget in the middle atmosphere, and cumulus convection has been identified as an important source of those nonstationary gravity waves. Among various convective systems, typhoon is a significant source of convective gravity waves [e.g., *Sato*, 1993; *Chane-Ming et al.*, 2002; *Dhaka et al.*, 2003; *Kim et al.*, 2005]. Recently, *Kim et al.* [2005] examined gravity waves generated by Typhoon Rusa (2002) using a mesoscale model and demonstrated that convective bands accompanied by the typhoon are the major source of inertio-gravity waves (IGWs). In their study, typhoon-induced IGWs in the stratosphere have dominant zonal wavelengths of 300–600 km, vertical wavelengths of 3–11 km, and periods of 6–11 hours. Gravity waves in the stratosphere have an asymmetric phase-speed spectrum mainly due to the critical-level filtering by the background wind, even though the convective forcing has a nearly symmetric spectrum.

[3] The characteristics of numerically simulated typhoon-induced gravity waves can differ depending on many factors, including individual typhoons and their development stages, synoptic environment, representation of physical processes, initialization methods, and analysis methods. Among the various physical processes, cloud and precipitation processes are crucial because latent heat release in deep cumulus convection is a primary energy source to drive a typhoon. Many previous studies indicate that simulated typhoon intensity and precipitation are sensitive to how cloud and precipitation processes are parameterized [e.g., *Baik et al.*, 1991; *Murata and Ueno*, 2000]. Since the pattern and intensity of typhoon-related rainbands affect induced gravity waves and simulated rainbands are sensitive to the choice of cloud parameterization, the characteristics of typhoon-induced gravity waves may be different according to cloud parameterization. This motivates the present study.

[4] In this study, we investigate the sensitivity of typhoon-induced gravity waves to subgrid-scale cumulus parameterization schemes. For this, we simulate Typhoon Rusa using a mesoscale model, described by *Kim et al.* [2005], with four different cumulus parameterizations and examine how the characteristics and propagation mechanism of induced gravity waves differ.

2. Typhoon Rusa and Experimental Design

[5] Typhoon Rusa moved northwestward after its formation on 23 August 2002, changed its direction to the north at 06 UTC 30 August, and landed on the Korean peninsula at 0630 UTC 31 August. Rusa had a minimum central pressure of 950 hPa.

[6] The Fifth-Generation Pennsylvania State University/National Center for Atmospheric Research (PSU/NCAR) Mesoscale Model (MM5) version 3 [*Dudhia et al.*, 2003] is used and except cumulus parameterization schemes the experimental setting is the same as given by *Kim et al.* [2005]. In this study, three additional simulations are conducted with Grell [*Grell*, 1993] (GR hereafter), Anthes-Kuo [*Kuo*, 1974; *Anthes*, 1977] (AK hereafter), and Betts-Miller [*Betts*, 1986; *Betts and Miller*, 1986] (BM hereafter) cumulus parameterizations. A total of four simulations are compared, including one with the Kain-Fritsch cumulus parameterization [*Kain and Fritsch*, 1993] (KF hereafter) performed by *Kim et al.* [2005]. The KF scheme is based on convective available potential energy, which is removed once convection is triggered. The KF scheme includes a cloud model considering entrainment/detrainment and convective scale updraft/downdraft. The GR scheme, which is based on available buoyant energy mass flux, considers convective scale updraft/downdraft. In the AK scheme, the convective heating is related to the vertically integrated moisture convergence. The BM scheme adjusts a local thermody-

[1]Department of Atmospheric Sciences, Yonsei University, Seoul, Korea.
[2]School of Earth and Environmental Sciences, Seoul National University, Seoul, Korea.

0094-8276/07/2007GL030592$05.00

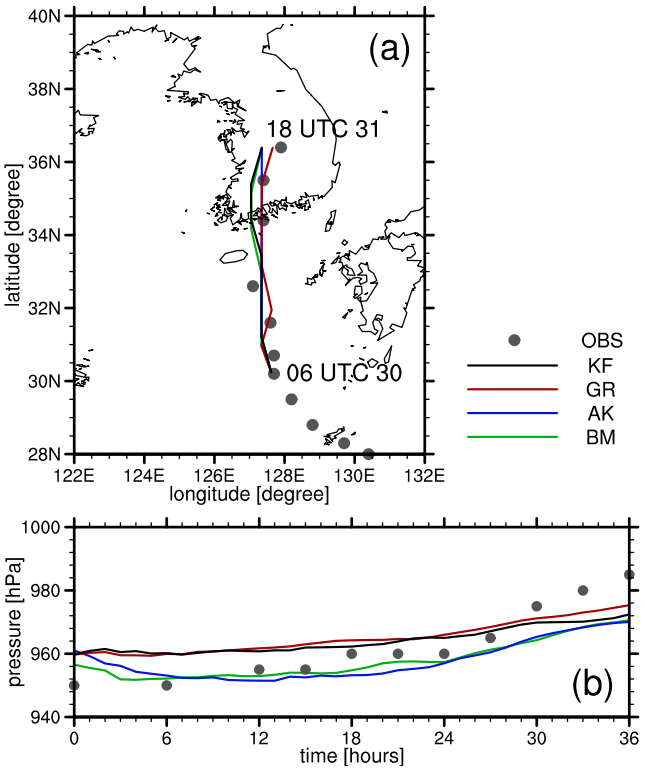

Figure 1. (a) Typhoon track and (b) minimum sea-level pressure. Filled circles indicate observations, and solid lines indicate simulations (black for the KF, red for the GR, blue for the AK, and green for the BM experiments).

namic profile toward the observed quasi-equilibrium thermodynamic profile with a relaxation time scale. In the deep convection part of the BM scheme, stability weight on moist adiabat and saturation pressure departure are important parameters. The numerical model is integrated for 36 hours from 06 UTC 30 August 2002, with a horizontal grid spacing of 27 km and 71 layers from the surface to 10 hPa. For details of experimental design, see *Kim et al.* [2005].

3. Results and Discussion

3.1. Track, Intensity, and Precipitation

[7] Figure 1 shows observed (filled circles) and simulated (solid lines) typhoon tracks and minimum sea-level pressures. All the simulated typhoon tracks represent the observed track fairly well. The data assimilation produces initial minimum sea-level pressures of 956 hPa in the BM experiment and about 960 hPa in the other experiments (the observed value is 950 hPa). The evolution of minimum sea-level pressure in the AK experiment (KF experiment) is similar to that in the BM experiment (GR experiment). The simulated typhoon is more intense in the AK and BM experiments than in the KF and GR experiments. The

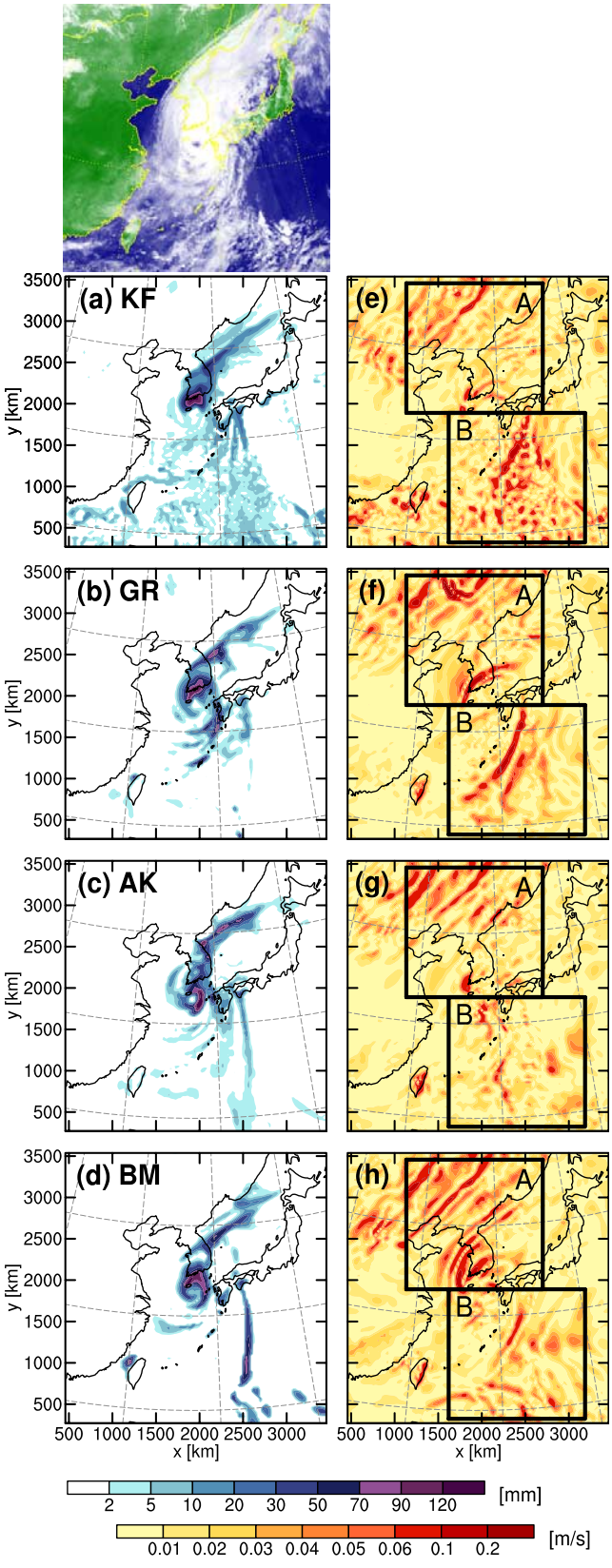

Figure 2. Six-hour accumulated precipitation amount (21 UTC 30–03 UTC 31 August 2002) in the (a) KF, (b) GR, (c) AK, and (d) BM experiments and the magnitude of vertical velocity at z = 17.4 km at t = 18 hours (corresponding to 00 UTC 31) in the (e) KF, (f) GR, (g) AK, and (h) BM experiments. Boxes in Figure 2, right, indicate domains where gravity wave analysis is conducted. Top (bottom) color bar is for Figure 2, left (right). Satellite image corresponding to this time is also shown in Figure 2, top.

weakening rate after landfall is slightly larger in the AK and BM experiments than in the KF and GR experiments, and it is smaller in all the experiments than in the observation.

[8] Figures 2a–2d show simulated precipitation amounts during 6 hours (21 UTC 30–03 UTC 31 August 2002). Although the simulated typhoon-related convection in all the experiments is comparable to the satellite image, there are some differences in the distribution of precipitation, especially in rainbands in the southeastern part of the typhoon. Precipitation in the eyewall and northern portion of the rainband, elongated northeastward from the main rainband, is largely from grid-scale precipitation, except in the AK experiment, where subgrid-scale precipitation is dominant. In the southeastern part of the typhoon, precipitation is dominated by subgrid-scale precipitation in the separate calculation of subgrid-scale precipitation and grid-scale precipitation (not shown). Therefore, precipitation structures are more sensitive to cumulus parameterization. In this area, the KF experiment shows a notably different structure with finer-scale convective cells in a wide area.

3.2. Characteristics of IGWs

[9] Figures 2e–2h show the magnitude of vertical velocity at z = 17.4 km at t = 18 hours (00 UTC 31 August) in each experiment. In all the experiments, perturbations propagate northwestward in the northwestern part (domain A) of the typhoon and southeastward in the southeastern part (domain B). Wave analyses are conducted in the same domains as given by *Kim et al.* [2005]. In domain A, perturbations are significant in the BM experiment compared with others, although precipitation in the BM experiment is not remarkable. In the AK experiment, in which the location of maximum precipitation in the eyewall is somewhat different from that in the other experiments (Figures 2a–2d), perturbations above eyewall are less distinct. The distribution of perturbations in domain B shows more variation among the experiments than that in domain A. In domain B, small-scale perturbations are notable in the KF experiment and band-type perturbations are notable in the GR experiment. In the AK experiment, perturbations are weak because of the small precipitation amount. In contrast to domain A, perturbations in the BM experiment are not larger than those in the KF and GR experiments, although the largest maximum precipitation occurs in the BM experiment. However, as will be shown in Figures 3 and 4, relatively high powers of waves appear at high frequency and short zonal wavelength in the BM experiment.

[10] Figure 3 shows power spectral densities (PSDs) of the vertical velocity as a function of zonal wavelength (left) and period (right) averaged in the forcing region (z = 3–15 km) and the stratosphere (z = 17–30 km) in the KF, GR, AK, and BM experiments during t = 1–36 hours. In the stratosphere, PSDs are calculated for components satisfying the vertical propagation condition of IGWs ($f < \hat{\omega} < N$), where $\hat{\omega}$ is the intrinsic frequency, f is the Coriolis parameter, and N is the Brunt-Vaisala frequency.

[11] In domain A, convective forcings have their dominant spectral power in similar zonal wavelengths (300–800 km) and periods (6–11 hours), except for shorter wavelengths in the AK experiment and a secondary peak at shorter period ($\sim$4 hours) in the BM experiment. The magnitude is largest (smallest) in the GR (AK) experiment. Total precipitations in domain A are similar in all the experiments, but the AK experiment produces the most precipitation from cumulus parameterization, while grid-scale precipitation is dominant in the other three experiments (especially in the GR experiment). It is found that PSD becomes large as grid-scale precipitation increases in domain A.

[12] Although the GR experiment shows the largest forcing magnitude in domain A, the amplitude of waves in the stratosphere is largest in the BM experiment. In the period spectrum of the BM experiment, the primary spectral peak in the stratosphere coincides with the secondary peak of the forcing. Based on the dispersion relation of IGW, waves with higher frequencies have longer vertical wavelengths for a given zonal wavenumber. According to *Marks and Eckermann*'s [1995] calculation, damping time scale increases with increasing vertical wavelength and frequency for the ranges of zonal and vertical wavelengths and period obtained in this study. Therefore, stratospheric waves with large amplitude in the BM experiment are those experienced less damping than lower frequency waves.

[13] In domain B, forcing magnitudes show more variability than in domain A, and spectral peaks exist at a zonal wavelength of about 200 km and periods of 3–11 hours. The BM experiment shows the largest forcing magnitude at zonal wavelengths larger than 100 km and periods longer than 7 hours. The KF experiment shows a relatively large forcing magnitude at shorter periods (less than 3 hours), as expected from Figure 2a. The AK experiment shows the smallest forcing magnitude at most zonal wavelength ranges, due to relatively weak convective activity after t = 12 hours when precipitation from subgrid-scale clouds (major precipitation source in the AK experiment) decreases rapidly with time. In spite of significantly different forcing magnitudes, stratospheric waves in all the experiments, except the AK experiment, have comparable amplitudes in similar zonal wavelengths (200–600 km) and periods (4–11 hours). In the KF experiment, perturbations with shorter periods (30 min–3 hours) are remarkable due to relatively large magnitude of the forcing at those periods across a wide zonal wavelength range.

[14] Figure 4 shows PSDs of the vertical velocity as a function of zonal phase speed (c_{px}) and height in domains A and B. Note different contour scales in the forcing region and in the stratosphere. In domain A, large magnitudes of the forcing in the GR and BM experiments (Figure 3) are due to westward-propagating components, which are stronger, especially in the GR experiment, than those in the KF and AK experiments. However, waves generated by those strong spectral components of the forcing ($c_{px} = -15$–25 m s^{-1}) are filtered out significantly by the background wind (shown as solid black lines) at their critical levels, at which the phase speed of wave equals the background wind speed, and damped in the stratosphere. There are relatively large-amplitude waves propagating westward faster than $c_{px} = -15$ m s^{-1} in the BM experiment. These waves are generated by high frequency components of forcing (Figure 3), which are relatively less damped. The waves propagating eastward faster than $c_{px} = 25$ m s^{-1} amplify with height, and they are stronger in the KF and BM experiments than in the GR and AK experiments. From PSD in the zonal wavenumber and ground-relative frequency domain (not shown), it is

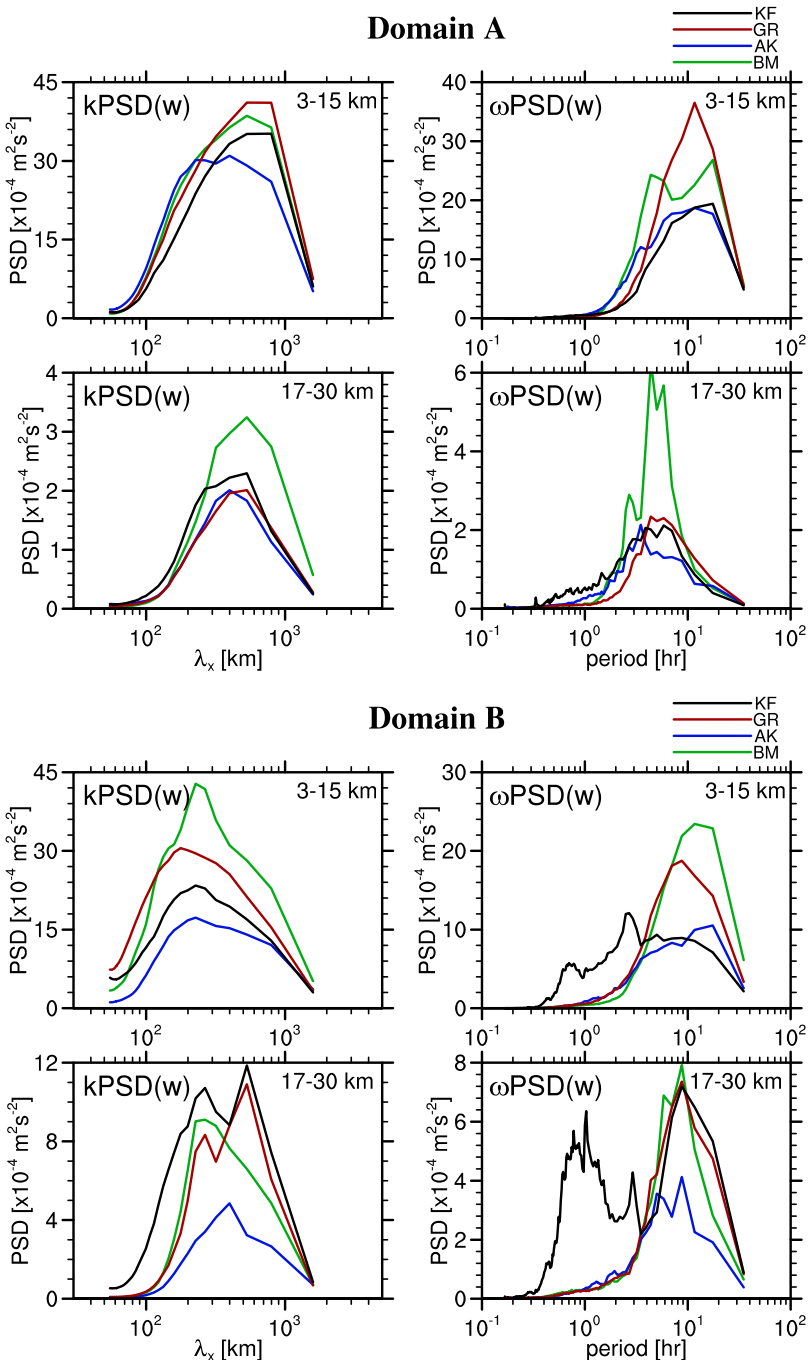

Figure 3. PSDs of the vertical velocity as a function of zonal wavelength (left) and period (right) in the KF (black), GR (red), AK (blue), and BM (green) experiments. (top) Domain A. (bottom) Domain B. Averages are taken over $z = 3-15$ km and $z = 17-30$ km. All PSDs are plotted in area-preserving forms.

found that this is due to stronger amplitude of eastward-propagating waves with periods of 4–6 hours in the BM experiment and shorter than 2 hours in the KF experiment.

[15] In domain B, convective forcing is stronger in the GR and BM experiments. In the stratosphere, waves propagating westward slower than 25 m s^{-1} are mostly filtered out by the easterly background wind. As a result, eastward-propagating waves are dominant, amplifying with height. The amplitude of waves with $c_{px} = 0-15$ m s^{-1} in the KF experiment is comparable to that in the GR and BM experiments, although forcing in the KF experiment is much smaller than in the GR and BM experiments and not larger than in the AK experiment. The reason is that in the KF experiment forcing at those phase speed (0–15 m s^{-1}) consists of relatively high frequencies and short zonal wavelengths, and waves generated by those forcing components are less damped when they propagate upward. Since wave amplitude is determined by a combination of amplification due to density reduction and dissipation due to turbulent and radiative dampings, less damped waves in the

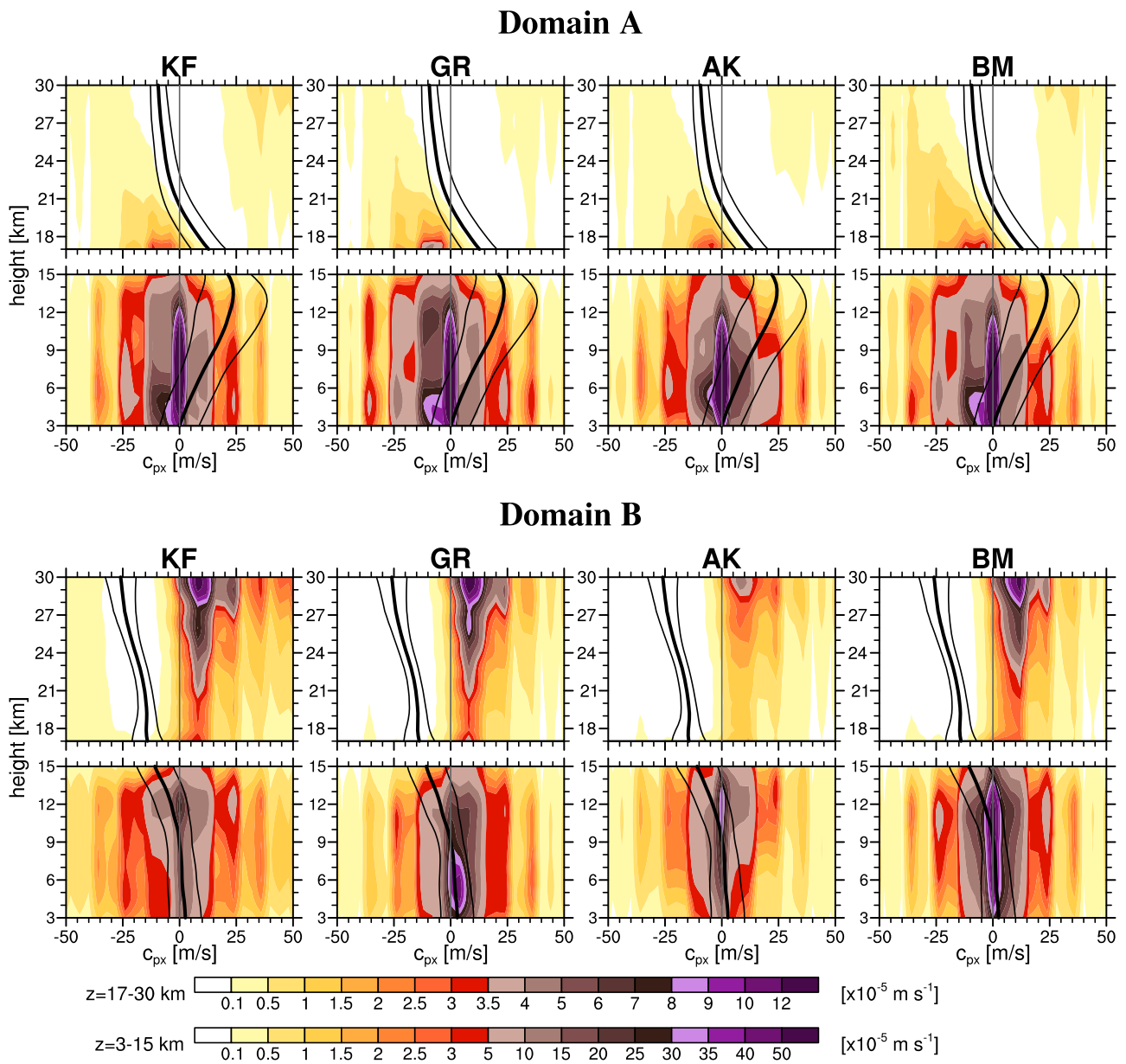

Figure 4. Vertical profiles of the vertical velocity spectrum as a function of zonal phase speed in domain A and domain B in the KF, GR, AK, and BM experiments. Thick solid lines denote the time-mean of the basic-state wind (U), and thin solid lines denote $U \pm \sigma$ (where σ is the standard deviation of U). Top (bottom) color bar is for the stratosphere (forcing region).

KF experiment will amplify more with height. That is why wave amplitude in the KF experiment is comparable to that in the GR and BM experiments with stronger forcing magnitude, and much larger than in the AK experiment with similar forcing magnitude. The amplitude of eastward-propagating waves with phase speeds faster than 15 m s^{-1} is proportional to the magnitude of the forcing at those phase speeds, and waves amplify with height without significant damping due to their relatively longer vertical wavelengths.

[16] In Figures 3–4, wave amplitude in the stratosphere is much smaller in domain A than in domain B, although the forcing magnitude is larger in domain A. This is because strong background wind shear filters out a large portion of waves generated by strong forcing in domain A. As discussed by *Kim et al.* [2005], asymmetric gravity wave spectrum in the stratosphere is mainly due to a critical-level filtering process, with contributions of a damping process and wave breaking in the nonfiltered region. Since cumulus parameterization does not induce a notable change in the background wind, at least in the present simulations, critical-level filtering occurs in almost the same phase-speed range regardless of the cumulus parameterizations used. Difference in the forcing spectrum in the nonfiltered region leads to a difference in wave dissipation, since a different wave spectrum can induce a different damping time scale. Potential wave breaking regions located at near-critical-level phase speeds in the KF experiment [*Kim et al.*, 2005], which are checked by comparison of momentum

flux with the saturation one followed by *Lindzen* [1981], are not so different among the experiments (not shown).

4. Concluding Remarks

[17] In this study, we examined the sensitivity of numerically simulated gravity waves induced by Typhoon Rusa (2002) to cumulus parameterizations, as an extension of *Kim et al.* [2005]. Wave characteristics and spectra induced by typhoons simulated with four cumulus parameterizations were compared. Although the difference in track and intensity according to cumulus parameterization is not larger than the error range between observation and simulation, differences in rainbands accompanied by typhoon, especially in the southeastern part of typhoon, are significant. As a result, forcing spectra calculated with vertical velocity in the troposphere are different, not only in the zonal wavenumber and frequency but also in their vertical structure.

[18] In general, there are two major factors that control the characteristics of gravity waves in the stratosphere: (i) the source spectrum in the troposphere and (ii) the wave propagation condition that is determined by the background wind and stability [*Chun et al.*, 2005]. In the two analysis domains considered in this study, the forcing spectrum in each experiment (with different cumulus parameterizations) has unique characteristics, although with common features (Gaussian-type forcing with a maximum value at near-zero phase speed). On the other hand, the background wind in each experiment is almost identical. In domain A (northwestern part of the typhoon), strong westerly wind shear from the midtroposphere to lower stratosphere filters out most of eastward and slowly westward-propagating waves, which are generated by major forcing components. Therefore, the difference between each experiment occurs in the nonfiltered waves for which the amplitude depends on damping time scale. For a case that can produce relatively strong forcing at high frequencies (BM experiment), wave amplitude is relatively large with less damped. On the other hand, in domain B (southeastern part of the typhoon), the background wind has a weak shear, and waves generated by major forcing components can propagate to the stratosphere without critical-level filtering. In this case, the difference in wave spectrum from each experiment is due to the magnitude and composition of the forcing spectrum, which influences wave amplification and damping processes. The characteristics and propagation mechanisms of gravity waves simulated by three additional cumulus parameterization schemes are generally similar to those in the previous study using a single cumulus parameterization scheme (KF) by *Kim et al.* [2005].

[19] **Acknowledgments.** SYK and HYC were supported by the Ministry of Science and Technology of Korea through the National Research Laboratory Program (M10500000114-06J0000-11410). JJB was supported by the Korea Foundation for International Cooperation of Science and Technology through the Global Partnership Program.

References

Anthes, R. A. (1977), A cumulus parameterization scheme utilizing a one-dimensional cloud model, *Mon. Weather Rev.*, *105*, 270–286.

Baik, J.-J., M. DeMaria, and S. Raman (1991), Tropical cyclone simulations with the Betts convective adjustment scheme. part III: Comparisons with the Kuo convective parameterization, *Mon. Weather Rev.*, *119*, 2889–2899.

Betts, A. K. (1986), A new convective adjustment scheme. part I: Observational and theoretical basis, *Q. J. R. Meteorol. Soc.*, *112*, 677–691.

Betts, A. K., and M. J. Miller (1986), A new convective adjustment scheme. part II: Single column tests using GATE wave, BOMEX, ATEX and arctic air-mass data sets, *Q. J. R. Meteorol. Soc.*, *112*, 693–709.

Chane-Ming, F., G. Roff, L. Robert, and J. Leveau (2002), Gravity wave characteristics over Tromelin Island during the passage of cyclone Hudah, *Geophys. Res. Lett.*, *29*(6), 1094, doi:10.1029/2001GL013286.

Chun, H.-Y., I.-S. Song, and T. Horinouchi (2005), Momentum flux spectrum of convectively forced gravity waves: Can diabatic forcing be a proxy for convective forcing?, *J. Atmos. Sci.*, *62*, 4113–4120.

Dhaka, S. K., M. Takahashi, Y. Shibagaki, M. D. Yamanaka, and S. Fukao (2003), Gravity wave generation in the lower stratosphere due to passage of the typhoon 9426 (Orchid) observed by the MU radar at Shigaraki (34.85°N, 136.10°E), *J. Geophys. Res.*, *108*(D19), 4595, doi:10.1029/2003JD003489.

Dudhia, J., D. Gill, K. Manning, W. Wang, C. Bruyere, S. Kelly, and K. Lackey (2003), PSU/NCAR mesoscale modeling system tutorial class notes and user's guide: MM5 modeling system, version 3, Mesoscale and Microscale Meteorol. Div., Natl. Cent. for Atmos. Res., Boulder, Colo.

Grell, G. A. (1993), Prognostic evaluation of assumptions used by cumulus parameterizations, *Mon. Weather Rev.*, *121*, 764–787.

Kain, J. S., and J. M. Fritsch (1993), Convective parameterization for mesoscale models: The Kain-Fritsch scheme, in *The Representation of Cumulus Convection in Numerical Models*, edited by K. Emanuel and D. J. Raymond, *Meteorol. Monogr.*, *24*, 165–170.

Kim, S.-Y., H.-Y. Chun, and J.-J. Baik (2005), A numerical study of gravity waves induced by convection associated with Typhoon Rusa, *Geophys. Res. Lett.*, *32*, L24816, doi:10.1029/2005GL024662.

Kuo, H. L. (1974), Further studies of the parameterization of the influence of cumulus convection on large-scale flow, *J. Atmos. Sci.*, *31*, 1232–1240.

Lindzen, R. S. (1981), Turbulence and stress owing to gravity wave and tidal breakdown, *J. Geophys. Res.*, *86*, 9707–9714.

Marks, C. J., and S. D. Eckermann (1995), A three-dimensional nonhydrostatic ray-tracing model for gravity waves: Formulation and preliminary results for the middle atmosphere, *J. Atmos. Sci.*, *52*, 1959–1984.

Murata, A., and M. Ueno (2000), The effects of different cumulus parameterization schemes on the intensity forecast of typhoon Flo, 1990, *J. Meteorol. Soc. Jpn.*, *78*, 819–833.

Sato, K. (1993), Small-scale wind disturbances observed by the MU radar during the passage of Typhoon Kelly, *J. Atmos. Sci.*, *50*, 518–537.

J.-J. Baik, School of Earth and Environmental Sciences, Seoul National University, San 56-1, Sillim-dong, Gwanak-gu, Seoul, 151–747, Korea.

H.-Y. Chun and S.-Y. Kim, Department of Atmospheric Sciences, Yonsei University, Shinchon-dong, Seodaemun-gu, Seoul 120–749, Korea. (chy@atmos.yonsei.ac.kr)